

GDSG: Graph Diffusion-based Solution Generation for Optimization Problems in MEC Networks

Ruihuai Liang, *Student Member, IEEE*, Bo Yang, *Member, IEEE*, Pengyu Chen, Zhiwen Yu, *Senior Member, IEEE*, Xuelin Cao, *Member, IEEE*, Mérouane Debbah, *Fellow, IEEE*, H. Vincent Poor, *Fellow, IEEE*, and Chau Yuen, *Fellow, IEEE*

Abstract—Optimization is crucial for MEC networks to function efficiently and reliably, most of which are NP-hard and lack efficient approximation algorithms. This leads to a paucity of optimal (ground-truth) data, constraining the effectiveness of conventional deep learning approaches. Most existing learning-based methods necessitate extensive optimal data and fail to exploit the potential benefits of suboptimal data that can be obtained with greater efficiency and effectiveness. Taking the multi-server multi-user computation offloading (MSCO) problem, which has been widely observed in systems such as Internet-of-Vehicles (IoV) and Unmanned Aerial Vehicle (UAV) networks, as a concrete scenario, we present a Graph Diffusion-based Solution Generation (GDSG) method. This approach is designed to work with suboptimal datasets while converging to the optimal solution large probably. We transform the network optimization issue into a distribution-learning problem and offer a clear explanation of learning from suboptimal training datasets. We build GDSG as a multi-task diffusion generative model utilizing a Graph Neural Network (GNN) to acquire the distribution of high-quality solutions. We use a simple and efficient heuristic approach to obtain a sufficient amount of training data composed entirely of suboptimal solutions. In our implementation, we enhance the backbone GNN and achieve improved generalization. GDSG also reaches nearly 100% task orthogonality, ensuring no interference between the discrete and continuous solution generation training objectives. We further reveal that this orthogonality arises from the diffusion-related training loss in GDSG, rather than the neural network architecture itself. The experiments demonstrate that GDSG surpasses other benchmark methods on both the optimal and suboptimal training datasets. Concerning the minimization of computation offloading costs, GDSG can achieve savings of up to 56.63% on the ground-truth training set and 41.07% on the suboptimal training set compared to the existing discriminative methods. The MSCO datasets has open-sourced at <http://ieeegdataport.org/13824>, as well as the GDSG algorithm codes at <https://github.com/qiyu3816/GDSG>.

Index Terms—Mobile edge computing, network optimization, computation offloading, generative AI, graph diffusion.

I. INTRODUCTION

IN various cutting-edge scenarios of Mobile Edge Computing (MEC) [1], [2], optimization demands are ubiquitous, such as trajectory optimization in Unmanned Aerial Vehicle

R. Liang, B. Yang, P. Chen, and Z. Yu are with the School of Computer Science, Northwestern Polytechnical University, Xi'an, Shaanxi, 710129, China. X. Cao is with the School of Cyber Engineering, Xidian University, Xi'an, Shaanxi, 710071, China. M. Debbah is with the Center for 6G Technology, Khalifa University of Science and Technology, P O Box 127788, Abu Dhabi, United Arab Emirates. H. V. Poor is with the Department of Electrical and Computer Engineering, Princeton University, Princeton, NJ 08544, USA. C. Yuen is with the School of Electrical and Electronics Engineering, Nanyang Technological University, Singapore.

Corresponding author: Bo Yang.

(UAV) networks [3]–[6], utility and latency optimization in edge networks for Federated Learning (FL) [7], [8], sum-rate and coverage optimization in Reconfigurable Intelligent Surface (RIS)-enhanced networks [9]–[13], efficiency optimization in Internet-of-Vehicles (IoV) [14]–[17], and other resource allocation tasks [18]–[25]. Despite the remarkable achievements of both numerical algorithms and Artificial Intelligence (AI) methods, a key challenge remains that a significant portion of these problems are NP-hard, with no efficient approximation algorithms currently available. This not only limits algorithms to suboptimal results, despite intensive manual design efforts, but also curtails the potential of AI-based methods. AI approaches typically require large-scale, optimally solved examples, which is unrealistic for problems that are inherently difficult to solve.

Fortunately, the success of generative AI has demonstrated its ability to generalize beyond the training data, offering a more robust AI approach to data quality. Large Language Models (LLMs) trained on limited texts have been shown to generate novel outcomes in response to diverse queries [26], [27], rather than merely reassembling the training data. Similarly, Generative Diffusion Models (GDMs) trained on image datasets can produce significantly different images under varying conditions [28], [29], rather than simply recalling training samples. Based on this, can we reasonably conclude that AI models for optimization do not necessarily need to rely on data composed of optimal solutions?

For many optimization problems in MEC that lack efficient solution methods, suboptimal solutions can often be more easily derived for many of these problems, while obtaining a sufficient number of optimal solutions is time-consuming and labor-intensive. For example, the multi-objective nature of some optimization problems [3]–[7], [10]–[12], [15]–[23] can be tackled through divide-and-conquer strategies to obtain suboptimal solutions, which are not only simple to implement but also computationally efficient. The core idea is to piece together existing simple algorithms to construct a complete suboptimal solution, which can obtain references from numerous previous studies. Many of these methods also feature low complexity, making them suitable for constructing large-scale datasets. While these suboptimal instances may not be very beneficial for current AI approaches, our work will leverage GDMs from generative AI to explore information and sample better solutions, with the potential to generate optimal solutions.

A. Motivation and Contribution

To address the aforementioned challenges, we attempt to use generative AI to learn from suboptimal datasets for solution generation in MEC network optimization problems. This is an approach that has not been explored before, and we will provide a detailed analysis of its effectiveness, along with experimental results.

We introduce a framework designed to acquire a parameterized solution distribution from imperfect solution samples. This is similar to the high-quality solution distribution in the DIMES [30], but it uses Deep Reinforcement Learning (DRL) instead of generative AI for optimization. Essentially, we view the feasible solution space of a given input as a distribution of solutions, with the optimal solution having the highest likelihood within this distribution. Subsequently, we parameterize the resulting solution distribution to facilitate distribution learning. Following this step, the parameterized distribution derived from the input can be concurrently sampled along with the approximation to the optimal solution. Distribution learning is an inherent capability of generative AI, with GDMs being among the most efficient [31], supporting various types of data patterns. To introduce a novel GDM-based approach for generating solutions to optimization problems and support as many applicable scenarios as possible, we consider the close relationship between optimization problems in MEC networks and graph-structured data, such as topology and routing trajectories [12], [18]–[20], [25]. Accordingly, we propose Graph Diffusion-based Solution Generation (GDSG), a method that solves problems at the graph level. Taking into account the multi-server multi-user setting in MEC networks, which may arise in scenarios like UAV and IoV networks, we model a multi-server multi-user computation offloading problem. We construct a suboptimal training set using heuristic methods and validate the performance of GDSG on this problem.

To the best of our knowledge, this is the first research attempt to build GDM-enabled solution generation method considering the training data limitations of complex optimization problems in MEC networks. The key contributions of our work are outlined below.

- We delve into the potential of suboptimal data samples and elucidate the rationale behind learning the solution distribution. We provide discussion about the convergence to the optimal solution and related conditions, with some insightful references summarized.
- We propose a graph optimization approach, trained solely on suboptimal data samples, demonstrating the capability to generate high-quality solutions and achieve optimal solutions for some inputs through parallel sampling. This alleviates the rely on laborious preparation of an optimal solution training set.
- We provide some practical insights from engineering implementation. By explicitly improving the Graph Neural Network (GNN) gating mechanism, the model's generalization ability across different graph scales is enhanced. Additionally, our analysis of multi-task simultaneous training reveals the orthogonality introduced by the diffusion model's loss objective, which results in negligible

interference between tasks.

B. Related works

1) *Learning-based optimization methods*: Current learning-based approaches to network optimization can be categorized based on their reliance on training data. The first category utilizes ground-truth datasets [5], [9], [20]–[23], [25], either created from scratch using standard solvers, brute force techniques, or directly drawn from open-source datasets. Nevertheless, open-source datasets have limited coverage, and the solvers' reliance on problem-specific assumptions and the high cost of dataset construction renders it impractical for new scenarios. The second category aims to reduce reliance on already solved datasets [6], [7], [14], [15], [17]–[19]. This approach primarily relies on reinforcement learning, guiding the model to explore improved policies through carefully crafted rewards and losses. However, this method heavily depends on expert knowledge and necessitates adjustments when the scenario changes.

2) *Graph diffusion and optimization*: As a common type of generative model, diffusion models involve a process of introducing noise and then learning to eliminate it. This method enables the model to predict and gradually recover the desired distribution by cyclically rectifying noise. An illustrative instance is the Denoising Diffusion Probabilistic Model (DDPM) [32], capable of producing distributions without constraints, while its variations can generate distributions based on specific conditions [33], [34].

Graph diffusion, on the other hand, involves learning and generating non-Euclidean graph-structured data by utilizing GNNs [35]. This method has shown success in solving combinatorial optimization problems like the Traveling Salesman Problem (TSP) and the Maximum Independent Set problem (MIS) with impressive outcomes [36], [37]. Specifically, T2T [37] enhances the sampled solutions by integrating gradient-guided generation based on DIFUSCO [36]. To date, graph diffusion models have proven beneficial by explicitly modeling graph structures to learn multi-modal distribution features.

Recent study [38]–[40] has delved into integrating diffusion models with network optimization, albeit primarily through practical cases in various optimization problems without concern for data robustness. Some works [41]–[43] also leverage GDMs as a stronger policy network in DRL, an emerging approach in the AI community, to address network optimization problems.

Different from the related works above, the proposed GDSG approach provides the implementation of graph-level modeling in complex optimization solving for MEC networks. Especially, our research leads the way in investigating the potential of suboptimal datasets utilized by GDMs and achieves a robust performance. Creating suboptimal datasets can be efficiently accomplished using basic heuristic algorithms which ensures the training data for GDSG. Based on the generative model's understanding of the solution distribution, optimal solution generation can be attainable through parallel sampling. Our implementation also allows multi-task optimization and enhanced generalization.

II. SYSTEM MODEL AND PROBLEM FORMULATION

With the development of systems such as UAV networks, RIS deployments, and IoV networks, the demand for more complex computational tasks has led to resource shortages on user devices. Computation offloading [2] has become an essential solution, and with the increasing number of edge devices, multi-server and multi-user offloading scenarios are becoming increasingly common [5]–[8], [10], [24].

A. System Model

Our system consists of edge servers and mobile users, where mobile users represent a unified abstraction of devices such as smartphones, drones, and vehicles. The number of servers and users in the system is variable, allowing for dynamic node mobility and the flexible joining or leaving of nodes based on task requirements.

1) *System components*: We formulate a binary computation offloading problem involving multiple servers and multiple users to minimize the weighted cost of delay and energy consumption, with the optimization variables of offloading decision and server computational resource allocation. As illustrated in Fig. 1, there exists a set of K edge servers, denoted as $\mathcal{S} = \{S_1, \dots, S_K\}$, and a set of M mobile users, denoted as $\mathcal{U} = \{U_1, \dots, U_M\}$ within the specified area. Due to the limited radio coverage of the edge servers, each user can only connect with a subset of edge servers. We assume that the uplink multiple access mechanism is orthogonal multiple access (OMA) [44], [45] to ensure interference-free wireless transmission.

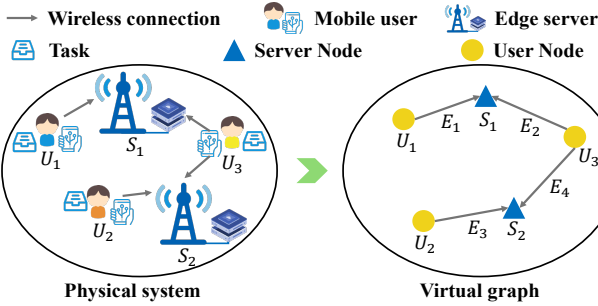


Fig. 1. System model of multi-server and multi-user computation offloading.

Abstracting the problem to a graph structure, we obtain the virtual graph of Fig. 1. Let $\mathcal{G}(\mathcal{V}, \mathcal{E})$ represent this directed acyclic graph, where $\mathcal{V} = \{\mathcal{U}, \mathcal{S}\}$. All feasible wireless connections are considered as directed edges from users to servers $\mathcal{E} = \{E_i(U_j, S_k) \mid \text{if } U_j \text{ has connection with } S_k\}$, where $L = |\mathcal{E}|$ and $i \in \{1, \dots, L\}, j \in \{1, \dots, M\}, k \in \{1, \dots, K\}$.

2) *Optimization variables*: We can observe that the dimension of the optimization variable is the same as the number of edges. Let $\mathcal{D} = \{D_1, \dots, D_i, \dots, D_L\}$ be the binary offloading decision of the mobile users \mathcal{U} , where $D_i \in \{0, 1\}$. So user U_j offloads to S_k if $E_i(U_j, S_k)$ exists and $D_i = 1$, otherwise U_j does not offload to S_k . If all offloading decisions for the edges associated with U_j are 0, it means that the computation task of U_j is executed locally rather than being offloaded.

Let $\mathcal{A} = \{A_1, \dots, A_i, \dots, A_L\}$ be the computational resource allocation for the mobile users \mathcal{U} , where $A_i \in [0, 1]$ represents the proportion of the total available computational resource from the server allocated to the user of E_i . Intuitively, we suppose that \mathcal{D} and \mathcal{A} determine the retention and weight of edges in the result, respectively.

3) *Binary offloading*: During the offloading optimization, each user is assumed to have an indivisible computing task, either executed locally or offloaded to a MEC server for execution. To intuitively formalize the relationship between edges and nodes, we define a binary function

$$\Upsilon(E_i, U_j) = \begin{cases} 1 & \text{if } U_j \text{ is the source node of } E_i \\ 0 & \text{otherwise} \end{cases} \quad \forall i \in \{1, \dots, L\}, \forall j \in \{1, \dots, M\}. \quad (1)$$

to determine whether U_j is the source node of the directed edge E_i . Therefore, the outgoing edges of a user node U_j should satisfy $\sum_{\Upsilon(E_i, U_j)=1} D_i \leq 1$.

In addition, the total amount of computational resources allocated to the tasks offloaded to a server cannot exceed the available computational resources of the server. We define a function

$$\Omega(E_i, S_k) = \begin{cases} 1 & \text{if } S_k \text{ is the destination node of } E_i \\ 0 & \text{otherwise} \end{cases} \quad \forall i \in \{1, \dots, L\}, \forall k \in \{1, \dots, K\}. \quad (2)$$

to determine whether S_k is the destination node of the directed edge E_i . Therefore, the incoming edges of a server node S_k should satisfy $\sum_{\Omega(E_i, S_k)=1} D_i A_i \leq 1$.

B. Weighted Cost of Delay and Energy Consumption

1) *Parameters of a user node for local computation*: Let $\mathbf{I} = \{I_1, \dots, I_L\}$, $\mathbf{V} = \{V_1, \dots, V_L\}$ and $\mathbf{F} = \{F_1^l, \dots, F_L^l\}$ be the input data sizes [bits], required computational resources [cycles] and available local computational resources [cycles per second] of the user tasks on each edge. Let $\alpha = \{\alpha_1, \dots, \alpha_L\}$ represent the weight of the task cost, where $\alpha_i \in [0, 1]$. So we have $\alpha \rightarrow 1$ if the delay cost is emphasized while the energy consumption cost is emphasized if $\alpha \rightarrow 0$. Clearly, the parameters related to local computation are the same for all outgoing edges of the same user node. So we have

$$I_i = I_j, V_i = V_j, F_i^l = F_j^l, \alpha_i = \alpha_j, \text{ if } E_i \text{ and } E_j \text{ have the same source node, } \forall i, j \in \{1, \dots, L\}. \quad (3)$$

2) *Cost of local execution*: For $E_i, i \in \{1, \dots, L\}$, its local execution time is calculated as $\tau_i = \frac{V_i}{F_i^l}$. Then, its local execution energy consumption can be obtained according to the energy consumption model [46] as $\omega_i^l = \kappa(V_i)^2 I_i$, where κ represents the energy efficiency parameter mainly depending on the chip architecture [47]. The weighted cost of local execution can be calculated as

$$C_i^l = \alpha_i \tau_i^l + (1 - \alpha_i) \omega_i^l, \quad \forall i \in \{1, \dots, L\}. \quad (4)$$

3) *Cost of transformation for offloading:* Let $\mathcal{H} = \{h_1, \dots, h_i, \dots, h_L\}$, $h_i \in [0, 1]$ be the channel gain and B be the channel bandwidth of the wireless connection represented by each edge. Let the power [W] of the uplink be P_t with additive Gaussian white noise of zero mean and variance N_0 . Then the uplink received signal-to-interference-plus-noise ratio (SINR) is $SINR_i = \frac{P_t(h_i)^2}{N_0 + P_t \sum(h_j)^2}$ where E_j and E_i has the same server node. In this way, the transmission rate of E_i is calculated as $r_i^u = B \log_2(1 + SINR_i)$. The weighted cost of transmission can be calculated as

$$\mathcal{C}_i^t = \alpha_i \frac{I_i}{r_i^u} + (1 - \alpha_i) P_t \frac{I_i}{r_i^u}, \quad \forall i \in \{1, \dots, L\}. \quad (5)$$

4) *Cost of offloading execution:* For the task execution on the server, let F be the total available computational resource [cycles/second] of the server and P_e be the processing power [W]. The weighted cost of fully-occupied offloading execution can be calculated as

$$\mathcal{C}_i^o = \alpha_i \frac{V_i}{F} + (1 - \alpha_i) P_e \frac{V_i}{F}, \quad \forall i \in \{1, \dots, L\}. \quad (6)$$

Therefore, the total offloading cost of E_i can be calculated as $D_i(\mathcal{C}_i^t + \frac{\mathcal{C}_i^o}{A_i})$.

5) *Additional parameters:* Since the computing task has a maximum tolerable delay τ_i [seconds], let $\rho_i \in [0, 1]$ represent the minimum computational resource allocation ratio required for offloading execution without timeout, and let $\psi_i \in \{0, 1\}$ represent whether the local execution will timeout or not. Only if the offloading was able to process without a timeout, $\rho_i > 0$. As a result, $\rho_i = 0$ if $\frac{I_i}{r_i^u} + \frac{V_i}{F} > \tau_i$ and $\rho_i = \frac{V_i}{(\tau_i - I_i/r_i^u)F}$ if $\frac{I_i}{r_i^u} + \frac{V_i}{F} \leq \tau_i$. Furthermore, $\psi_i = 0$ if the local execution will timeout, $\psi_i = 1$ otherwise. Therefore, we use $(\mathcal{C}_i^l, \mathcal{C}_i^t, \mathcal{C}_i^o, \rho_i, \psi_i)$ as the 5-dimensional edge feature in \mathcal{G} to represent computing tasks, communication parameters, and resource settings.

C. Weighted Cost Minimization Problem

According to Eqs. (4), (5) and (6), the minimization problem of one round offloading optimization can be formulated as

$$\mathbb{P} : \min_{\{\mathcal{D}, \mathcal{A}\}} \sum_{i=1}^L (1 - D_i) \mathcal{C}_i^l + D_i (\mathcal{C}_i^t + \frac{\mathcal{C}_i^o}{A_i}),$$

s.t. **C1** : $D_i \in \{0, 1\}, \forall i \in \{1, \dots, L\}$, (7a)

C2 : $A_i \in [0, 1], \forall i \in \{1, \dots, L\}$, (7b)

C3 : $\sum_{\Upsilon(E_i, U_j)=1} D_i \leq 1, \forall j \in \{1, \dots, M\}$, (7c)

C4 : $\sum_{\Omega(E_i, S_k)=1} D_i A_i \leq 1, \forall k \in \{1, \dots, K\}$. (7d)

Let $\{\mathcal{D}^*, \mathcal{A}^*\}$ be the optimal solution for the given input parameters, the problem \mathbb{P} can be transformed from the original Mix-Integer Non-Linear Programming (MINLP) to a multi-task graph optimization. It is important to note that although \mathbb{P} is formally an MINLP problem, existing solvers are not equipped to handle such a challenging graph-structured problem. For example, GEKKO [48] only accepts vector-based problem and constraint formulations, and its solution time for

MINLP problems is excessively long. With the node features that represent node types (e.g., 1 represents a server node and 0 represents a user node) and edge features that explicitly denote objective and constraint, the graph-based problem formulation approach can provide rich information and is transferable to alternative problems.

III. PROBLEM ANALYSIS

In this section, we will provide an introduction to the principles and concepts of solution distribution learning, explicitly highlighting the robustness of this learning objective with respect to solution quality, thereby supporting the learning from suboptimal solution data.

A. Why and How to Learn the Solution Distribution?

For the optimization problem in Eq. (7), the existing methods generally obtain truth input-solution paired samples like (x, y^*) , $x \in \mathcal{X}, y^* \in \mathcal{Y}_x$, \mathcal{X} and \mathcal{Y}_x represent the input parameter space and the feasible solution space for a given x , respectively. By referring to and extending the definition of parametrized solution space in DIMES [30], we parametrize the solution space with a continuous vector $\theta \in \mathbb{R}^N$, where N represents the dimension of the optimization variable, and estimate the probability of each feasible solution y as

$$p_\theta(y|x) \propto \exp\left(\sum_{i=1}^N y_i \theta_i\right) \quad \text{s.t. } y \in \mathcal{Y}_x, \quad x \in \mathcal{X}. \quad (8)$$

where p_θ is an energy function indicating the probability of each solution over the feasible solution space. We first consider the discrete solution space that y is an N -dimensional vector with $y_i \in \{0, 1\}$, and the higher value of θ_i denotes a higher probability that y_i is consistent with y^* . There exists θ^* be the optimal parametrization of the solution space for a given $x \in \mathcal{X}$ if θ^* satisfies $p_{\theta^*}(y^*|x) = 1$.

Accordingly, θ describes a solution distribution. Taking the discrete binary classification problem as an example, for the optimal solution y^* , it is parametrized as a binomial distribution, i.e., $\theta_{i0}^* = 0, \theta_{i1}^* = 1$ if $y_i^* = 1$, and $\theta_{i0}^* = 1, \theta_{i1}^* = 0$ if $y_i^* = 0$, where θ_{i0} represents the probability that $y_i = 0$ and vice versa. Therefore, (x, y^*) can be replaced by (x, θ^*) for learning.

Although learning θ^* can guarantee the results, it is obvious that θ^* is too sharp to be different from discriminative training, which makes parametrization redundant. For the NP-hard problems considered in this paper, it is impossible to efficiently obtain a large number of truth samples for discriminative supervised training. However, suboptimal solutions are much easier to obtain.

Let (x, y') be a suboptimal solution for a given x , and (x, θ') be the parametrization. To avoid verbosity, we will not introduce the definition of the gap between suboptimal solutions and the optimal solution here and leave it in Sec. III-B. We know that suboptimal parameterizations are not unique. For example, taking $\theta'_1 = (0.9, 0.1), \theta'_2 = (0.95, 0.05)$ for $\theta^* = (1, 0)$, where repeated sampling of $p_{\theta'_1}(y|x)$ or $p_{\theta'_2}(y|x)$ can easily hit the optimal solution. Therefore, let Y'_x

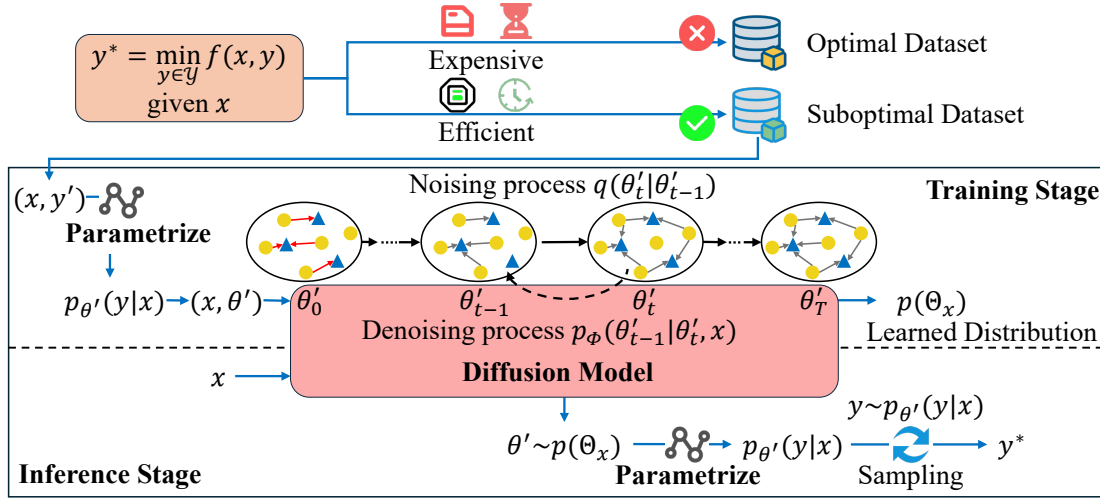


Fig. 2. Framework for training the diffusion generative model with suboptimal dataset to achieve the optimal solution generation.

be the set of suboptimal solutions for x , and Θ_x be the set of suboptimal parameterizations.

For the continuous solution space, it is impossible to make the calculated solution completely equal to the y^* because of the infinite precision. As a discussion example, we parametrize y^* using sharp Laplace distribution. For example, for y_i^* , $\theta_i^* = y_i^*$ for $\text{Laplace}(\theta_i^*, \text{scale_factor})$, smaller scale_factor means sharper probability density function and the probability of y^* is the largest and tends to 1. Thus, we can obtain the continuous solution space's Y'_x and Θ_x .

Consequently, when given only a dataset of suboptimal solutions, learning the parametrization of the solution space to sample feasible solutions can lead to the optimal solution. Specifically, the model aims to learn $p(\Theta_x)$ to obtain $\theta' \sim p(\Theta_x)$ and sample feasible solutions $y \sim p_{\theta'}(y|x)$, achieving the optimal solution (see Fig. 2).

B. Convergence to the Optimal Solution

In the previous sections, we have successfully transformed the goal into learning and sampling $p(\Theta_x)$. In this section, we discuss the quality requirements of suboptimal solutions and the generation convergence to optimal solutions.

1) *Gap between suboptimal and optimal parameterizations:* Let $(x, \theta^*), x \in \mathcal{X}$ and $(x, \theta'), \theta' \sim p(\Theta_x)$. Although it is not possible to precisely quantify the magnitude of suboptimal perturbations, for the sake of initial discussion, we assume that the perturbations caused by suboptimal solutions are smoothly random and the mean $\mathbb{E}(\Theta_x) = \mu = \theta^*$ holds. With $\mathbb{V}(\Theta_x) = \sigma^2$ as the variance of $p(\Theta_x)$, we can get Chebyshev's inequality [49] as below

$$p\{|\theta' - \theta^*| \geq \epsilon\} \leq \frac{\sigma^2}{\epsilon^2}, \forall \epsilon > 0. \quad (9)$$

Eq. (9) presents the impact of the model solution generation variance and the quality of suboptimal solutions on the gap between the learned suboptimal and optimal parameterizations. The probability that the parametrized θ' of the model output falls outside the ϵ -neighborhood of θ^* can be small. However,

since the generation variance of the diffusion model cannot be theoretically quantified, we conduct simulations and analysis in the experimental section to explore this further.

2) *Expectation of hitting y^* :* For the N -dimensional binary classification problem in the discrete solution space, we have $|\theta_i - \theta_i^*| = \epsilon, \theta \in \dot{U}(\theta^*, \epsilon), i \in \{1, \dots, N\}$. With $\theta_i^* = 1$ generally, the probability of hitting y^* in a single sampling is $(1 - \epsilon)^N$ with independent variables in each dimension. The probability of hitting y^* at least once in n samplings can be calculated as $1 - [1 - (1 - \epsilon)^N]^n$, which is finite.

For the N -dimensional regression problem in the continuous solution space, let $\theta \in \dot{U}(\theta^*, \epsilon)$ have mean $\mu + \epsilon$ and variance γ^2 . Keeping the implication of the mean consistent, the parametrized distribution can be independent of the diffusion model sampling. In our discussion, we use Gaussian distribution $\mathcal{N}(\mu + \epsilon, \gamma^2)$ for feasible solution sampling. Take the tolerable gap as $\delta > 0$, the probability of falling $[y_i^* - \delta, y_i^* + \delta]$ in a single sampling is

$$P_i = P(\mu_i - \delta \leq y_i \leq \mu_i + \delta) = \int_{\mu_i - \delta}^{\mu_i + \delta} (1/\sqrt{2\pi\gamma_i^2}) \exp\left(-\frac{(y - (\mu_i + \epsilon))^2}{2\gamma_i^2}\right) dy, \quad (10)$$

where $y_i \sim \mathcal{N}(\mu_i + \epsilon, \gamma_i^2), \mu_i = y_i^*$.

Also with independent variables in each dimension, the probability of hitting y^* at least once in n samplings can be calculated as $1 - (1 - \prod_{i=1}^N P_i)^n$, which is finite.

Therefore, given an ϵ -neighborhood of θ^* as $\dot{U}(\theta^*, \epsilon)$, and θ is taken from $\dot{U}(\theta^*, \epsilon)$. Let $q(\theta^n)$ be the probability of hitting y^* at least once in n samples $y \sim p_\theta(y|x)$, if ϵ in Eq. (9) makes the gap between θ' and θ^* sufficiently small, a finite number of samples n can make the expectation $\mathbb{E}(q(\theta^n)) \approx 1$.

3) *The lower bound on the number of samples:* To demonstrate the impact of N and n on the expectation of hitting y^* , we provide Fig. 3 and give the detailed calculation settings in Sec. V-B. Based on the above discussion, we can give a lower bound on n that makes $\mathbb{E}(q(\theta^n)) \approx 1$ hold. By simplifying

$p_\epsilon = p\{|\theta' - \theta^*| \geq \epsilon\}$ and letting $a > 0$ and $a \rightarrow 0$, we can multiply both sides of Eq. (9) by $1 - [1 - (1 - \epsilon)^N]^n$ to obtain

$$(1 - p_\epsilon)[1 - (1 - (1 - \epsilon)^N)^n] > (1 - \frac{\sigma^2}{\epsilon^2})[1 - (1 - (1 - \epsilon)^N)^n] + a, \quad \forall \epsilon > 0, \quad (11)$$

where $1 - [1 - (1 - \epsilon)^N]^n > 0$ does not change the sign of the inequality, and the left side represents the probability that $\theta \in U(\theta^*, \epsilon)$ and $\mathbb{E}(q(\theta^n)) \approx 1$ occur simultaneously. For a given a , $p(\Theta_x)$ in our problem is almost impossible to be the three-point distribution required by the equality condition in Chebyshev's inequality¹, so the sign ' \geq ' can be directly replaced by ' $>$ ', thus an invalid inequality will not appear because $a \rightarrow 0$.

With the Eq. (9) holds, we observe that $p_\epsilon \leq \frac{\sigma^2}{\epsilon^2}$. After transposition and simplification, we can get the lower bound on n for the discrete solution space:

$$n > \frac{\ln(\frac{a}{p_\epsilon - \sigma^2/\epsilon^2} + 1)}{\ln(1 - (1 - \epsilon)^N)}, \quad \forall \epsilon > 0. \quad (12)$$

For a continuous solution space, we use $1 - (1 - \prod_{i=1}^N P_i)^n$ to replace $1 - (1 - (1 - \epsilon)^N)^n$ and the lower bound can be calculated as

$$n > \frac{\ln(\frac{a}{p_\epsilon - \sigma^2/\epsilon^2} + 1)}{\ln(1 - \prod_{i=1}^N P_i)}, \quad \forall \epsilon > 0. \quad (13)$$

To demonstrate the impact of N on the lower bound on n that supports $\mathbb{E}(q(\theta^n)) \approx 1$, we illustrate it in Fig. 3 and the detailed settings in Sec. V-B.

Based on the above discussion, we explain that the model is capable of learning a solution distribution θ' that is sufficiently close to the optimal parametrization θ^* . Furthermore, within a finite number of samples, the expectation of hitting the optimal solution at least once can approach 1. Exploratively, we provide a lower bound expression (Eq. (12), Eq. (13)) for the number of samples n that supports this expectation approaching 1. These equations are further studied by experiments and model results, thereby providing valuable basis and reference conditions.

IV. THE PROPOSED GDSG ALGORITHM

With the solution distribution parametrization provided, the core theoretical concept in Sec. III is to establish a model capable of generating $\theta' \sim p(\Theta_x)$ for a given x . Generative models aim to model the joint distribution of inputs and outputs, $P(\Theta_x, x)$, in contrast to discriminative models, which learn the conditional probability distribution $P(\Theta_x|x)$. Consequently, the generative model uses the implicitly learned $P(\Theta_x|x)$ as a guide to generate $\theta' \sim p(\Theta_x)$ in conditional generation [33], thereby enhancing the likelihood of producing high-quality outputs. To address the graph optimization problem outlined in Sec. II and implement the approach outlined in Sec. III, we propose a graph diffusion generative model for solution generation.

¹https://en.wikipedia.org/wiki/Chebyshev%27s_inequality.

A. Graph Diffusion for Solution Generation

From the perspective of variational inference, the general diffusion framework consists of a forward denoising process and a learnable reverse denoising Markov process [32], [50], [51].

As described in Sec. II, for an input $\mathcal{G}(\mathcal{V}, \mathcal{E})$, the optimal solution to the multi-server multi-user computation offloading problem can be expressed as $\{\mathcal{D}^*, \mathcal{A}^*\}$. Next, we introduce the diffusion generation of \mathcal{D}^* and \mathcal{A}^* in the following two aspects: discrete solutions and continuous solutions generation, and the output solutions are represented by y and y for discrete and continuous solution respectively.

1) *Discrete Solution Diffusion*: For discrete solution $y \in \mathcal{Y}$, it is parametrized as a one-hot vector that $y \in \{0, 1\}^{L \times 2}$. Given an instance (\mathcal{G}, y) , diffusion takes y as the initial solution y_0 to perform the denoising process, also known as the diffusion process, gradually introducing noise to obtain a series of variables $y_{1:T} = y_1, \dots, y_T$ with T as the diffusion steps. The specific denoising process can be formalized as $q(y_{1:T}|y_0) = \prod_{t=1}^T q(y_t|y_{t-1})$. The model learns the noise distribution from this process, enabling it to denoise from a given initial noise distribution to a target distribution. The denoising process actually starts from y_T and performs adjacent step denoising from y_t to y_{t-1} with \mathcal{G} as the condition. The denoising process can be expressed as $p_\Phi(y_{0:T}|\mathcal{G}) = p(y_T) \prod_{t=1}^T p_\Phi(y_{t-1}|y_t, \mathcal{G})$, where Φ represents the model parameters. The ideal result of diffusion model training is $p_\Phi(y|\mathcal{G}) = q(y|\mathcal{G})$, and to fit the original data distribution, the variational upper bound of the negative log-likelihood is generally used as the loss objective

$$\begin{aligned} \mathcal{L} = & \mathbb{E}_q[-\log p_\Phi(y_0|y_1, \mathcal{G}) \\ & + \prod_{t>1} D_{KL}[q(y_{t-1}|y_t, y_0) \parallel p_\Phi(y_{t-1}|y_t, \mathcal{G})]] + C, \end{aligned} \quad (14)$$

where D_{KL} represents Kullback–Leibler divergence, a measure of the difference between two distributions, and C represents a constant.

In the forward noising process, y_t is multiplied by \mathbf{Q}_t to obtain y_{t+1} , where $\mathbf{Q}_t = \begin{bmatrix} (1 - \beta_t) & \beta_t \\ \beta_t & (1 - \beta_t) \end{bmatrix}$ is the transition probability matrix [35], [52]. The operation $y\mathbf{Q}$ converts and adds noise to the one-hot vector of each element $y_i \in \{0, 1\}^2$, with β_t controlling the noise scale as the corruption ratio. Specifically, $\prod_{t=1}^T (1 - \beta_t) \approx 0$ ensures that $y_T \sim \text{Uniform}(\cdot)$. Let $\bar{\mathbf{Q}}_t = \mathbf{Q}_1 \mathbf{Q}_2 \dots \mathbf{Q}_t$, the single-step and t-step marginals of the noising process can be formulated as

$$\begin{aligned} q(y_t|y_{t-1}) &= \text{Cat}(y_t; \mathbf{p} = y_{t-1}\mathbf{Q}) \quad \text{and} \\ q(y_t|y_0) &= \text{Cat}(y_t; \mathbf{p} = y_0\bar{\mathbf{Q}}_t), \end{aligned} \quad (15)$$

where $\text{Cat}(\cdot)$ represents a categorical distribution, which can be any discrete distribution. Here, in line with experience setting [35], a Bernoulli distribution is applied.

According to Bayes' theorem, the posterior can be calculated as

$$\begin{aligned} q(y_{t-1}|y_t, y_0) &= \frac{q(y_t|y_{t-1}, y_0)q(y_{t-1}|y_0)}{q(y_t|y_0)} \\ &= \text{Cat}(y_{t-1}; \mathbf{p} = \frac{y_t \mathbf{Q}_t^T \odot y_0 \mathbf{Q}_{t-1}^T}{y_0 \mathbf{Q}_t^T y_t^T}), \end{aligned} \quad (16)$$

where \odot denotes element-wise multiplication.

The model is trained to predict the distribution $p_\Phi(\tilde{y}_0|y_t, \mathcal{G})$, allowing the denoising process to be obtained by substituting the y_0 in Eq. (16) with the estimated \tilde{y}_0

$$p_\Phi(y_{t-1}|y_t) \propto \sum_{\tilde{y}_0} q(y_{t-1}|y_t, \tilde{y}_0) p_\Phi(\tilde{y}_0|y_t, \mathcal{G}). \quad (17)$$

2) *Continuous Solution Diffusion*: For the continuous solution $y \in [0, 1]^L$, continuous diffusion models [32]–[34] can be directly applied without parametrization. Unlike previous studies [36], [37], which rescales discrete data in continuous diffusion for discrete data generation [53], our multi-task generation approach uses continuous diffusion for continuous solutions.

The noising and denoising process formulas for continuous diffusion are essentially the same as those for discrete diffusion, and the loss objective is similar to Eq. (14). The primary difference is that the transition probability in continuous diffusion is Gaussian rather than categorical. Therefore, let β_t be the corruption ratio, the single-step and t-step marginals of the noising process for continuous diffusion can be formulated as

$$\begin{aligned} q(y_t|y_{t-1}) &= \mathcal{N}(y_t; \sqrt{1 - \beta_t} y_{t-1}, \beta_t \mathbf{I}) \\ q(y_t|y_0) &= \mathcal{N}(y_t; \sqrt{(1 - \beta_t)} y_0, (1 - \sqrt{(1 - \beta_t)}) \mathbf{I}), \end{aligned} \quad (18)$$

where $\sqrt{(1 - \beta_t)} = \prod_{t=1}^T (1 - \beta_t)$, and $\prod_{t=1}^T (1 - \beta_t) \approx 0$ ensures that $y_T \sim \mathcal{N}(\cdot)$. Similar to Eq. (16), the posterior can be calculated as

$$q(y_{t-1}|y_t, y_0) = \frac{q(y_t|y_{t-1}, y_0)q(y_{t-1}|y_0)}{q(y_t|y_0)}. \quad (19)$$

The model is trained to predict the Gaussian noise $\tilde{\epsilon}_t = f_\Phi(y_t, t, \mathcal{G})$. Given that $\tilde{\epsilon}_t = (y_t - \sqrt{(1 - \beta_t)} y_0) / \sqrt{1 - (1 - \beta_t)}$, the denoising process can be obtained by substituting the y_0 in Eq. (19) with an estimation

$$p_\Phi(y_{t-1}|y_t) \propto q(y_{t-1}|y_t, \frac{y_t - \sqrt{1 - (1 - \beta_t)} f_\Phi(y_t, t, \mathcal{G})}{\sqrt{(1 - \beta_t)}}). \quad (20)$$

B. GNN-based Diffusion Model

In Sec. II, we model the computation offloading in the MEC network as a graph optimization problem to enhance the model's versatility in network optimization. The optimization variables are represented as discrete solutions for edge selection and continuous solutions for edge weights, corresponding to offloading decisions and computational resource allocation ratios. For the model prediction objectives in Eq. (17) and Eq. (20), theoretically, any neural network structure can be

employed. We use a convolutional GNN with a specified edge gating mechanism, which is designed to mitigate the effects of padding edges [54], [55]. We employ a multi-task approach to expand the model, supporting the prediction objectives in Eq. (17) and Eq. (20).

The core operation of the GNN layer involves transferring or aggregating edge and node feature information locally or globally [56], with various options for aggregation operation. Additionally, the edge gating mechanism controls the nonlinear activation of edge features before aggregation using off-the-shelf functions. Specifically, the GNN takes the current step t , the feature graph \mathcal{G} , and the current solution with the same data structure as \mathcal{G} as input. For known node and edge feature dimensions, the model embeds them into a latent space of preset dimensions (usually high dimensions) and performs recursive information transfer and aggregation in this latent space. Information extraction and fusion in the latent space can be considered the source of the GNN's permutation-invariance.

However, we noticed that the existing works [36], [37] using convolutional GNN only considered fully connected input graphs for the TSP and MIS problems, whereas most graph optimization problems are not fully connected. In dense adjacency matrix and sparse edge list graph data structures, some edges may not exist, which we refer to as padding edges. The feature encoding of these padding edges can have unpredictable (and often adverse) effects on the iteration of the GNN in the latent space. This issue is not well addressed by previous works.

We investigated this problem during our experiments, as detailed in Sec. V-D. Specifically, the feature embedding of padding edges is non-zero. The input graphs of different sizes may have varying proportions of padding edges, and their influence is difficult to generalize or eliminate through simple linear or nonlinear gating. Changing the aggregation method (e.g., sum, mean, max) offers little help. Moreover, we considered setting the original features of padding edges to zero and setting the bias of the edge feature embedding layer to zero simultaneously. However, this approach could adversely affect the embedding of normal edges and might still not completely distinguish padding edges from normal edges in some cases.

To address this, we design a gating mechanism that can mitigate the effects of padding edges, inspired by the spirits that the generalization performance of GNNs benefits from explicit redesign [54], [56]. We add a one-dimensional 0-1 variable to the edge feature to indicate whether an edge is a padding edge. This variable multiplies the original gating result, completely eliminating the influence of meaningless hidden features from padding edges.

At this point, our GNN model has been extended to multi-task capabilities and improved in generalization for both fully connected and non-fully connected graphs. Additionally, as an anisotropic GNN handling directionally dependent features, our model is not limited to the directed graph problem in Sec. II and can be directly applied to undirected graphs. GNNs inherently offer versatility, allowing a single trained model to handle graphs of different scales for the same problem. Moreover, the settings of node and edge features can be

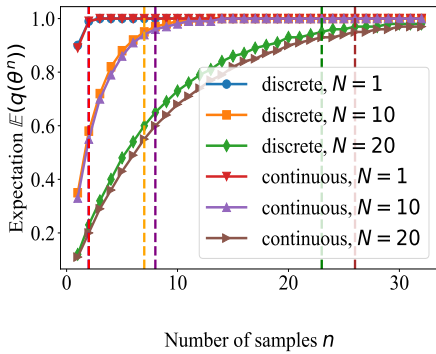


Fig. 3. The expectation of hitting y^* for different number of samples n and variable dimension N . The dotted lines represent the lower bounds on n , where the red and blue dotted lines coincide.

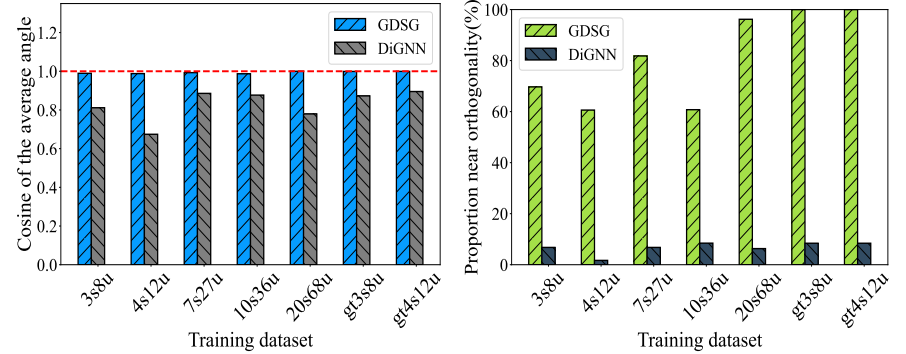


Fig. 4. Left: The cosine value of the overall average of all relevant parameters (The closer to 1, the better the orthogonality). Right: The proportion of the orthogonal vector for a given range in a training step (The closer to 100%, the better the orthogonality).

flexibly adjusted to support various MEC tasks.

C. Multi-Task Generation and Denoising Schedule

Our model performs multi-task generation, denoising both the target discrete solution and the continuous solution. In multi-task learning, negative competition between tasks can lead to poor convergence. However, we find that the discrete and continuous diffusion tasks largely satisfy the metric of inter-task gradient direction orthogonality, a key goal in specialized multi-task learning research [57]–[59]. Our experiments reveal that the gradient vectors calculated on the same layer parameters for the two tasks are almost orthogonal. Details are provided in Sec. V-C. A comparison using the same neural network structure for discriminative training confirms that this orthogonality is not inherent to the network architecture. We believe this characteristic is unique to the training loss objectives of discrete and continuous diffusion, a phenomenon not yet reflected in existing multi-task learning research on diffusion models [60]–[62].

Conventionally, we employ DDIM to accelerate the denoising inference of the diffusion model [63]. DDIM rewrites the denoising formula, leveraging the independence of marginal probabilities between two adjacent steps in the original process. This approach significantly reduces the number of inference steps while maintaining denoising performance. For discrete diffusion, we use a similar method [35].

V. EXPERIMENTS

To verify our proposed methods and models, we build instances of the multi-server multi-user computation offloading problem at various scales. We first provide targeted simulation validation for the approach outlined in Sec. III, then we conduct a gradient analysis for multi-task orthogonality and compare GDSG with a discriminative model of the same neural network structure. Finally, we compare GDSG with multiple baselines in terms of cost metrics.

A. Experiments Settings

1) *Datasets*: We tentatively tried using GEKKO [48] solver to generate non-graph data for a single server, but the solution

time for a single solve of a four-node MINLP problem reached several seconds. Moreover, GEKKO cannot handle graph structure data. As a result, we use a heuristic algorithm with polynomial time complexity to generate suboptimal datasets for the computation offloading problem in Sec. II. The Minimum Cost Maximum Flow (MCMF) algorithm, applied to random heuristic initialization of edge weights, efficiently finds optimal edge selection results and provides high-quality suboptimal solutions (solving a single instance with 80 nodes in 0.6sec). Since an optimal solver is not available, we use exhaustive methods to generate small-scale ground-truth datasets but the time complexity is very high (over 30sec for a single instance of 80 nodes).

We generate 14 training datasets with varying problem scales: lq3s6u, lq3s8u, lq4s10u, lq4s12u, lq7s24u, lq7s27u, lq10s31u, lq10s36u, lq20s61u, lq20s68u, gt3s6u, gt3s8u, gt4s10u, and gt4s12u. For example, “lq3s6u” represents a suboptimal dataset with 3 servers and 6 users at relatively low-quality, while “gt3s6u” represents the optimal dataset with 3 servers and 6 users at ground-truth. Our scale setting considers the radio coverage of edge servers, ensuring each user can only connect to a subset of servers. Ultra-sparse and ultra-dense settings lacking practical significance for computation offloading are not considered. Each suboptimal training dataset contains either 60000 or 80000 samples, while each optimal training dataset contains 2000 samples due to the complexity. The testing sets consist of 10 different problem scales: gt3s6u, gt3s8u, gt4s10u, gt4s12u, gt7s24u, gt7s27u, gt10s31u, gt10s36u, gt20s61u, and gt20s68u. We provide thousands of test instances for testing sets. None of the test samples appeared in the training set.

2) *Model Settings*: The main hyperparameters include diffusion_steps, GNN_layer_num, hidden_dim, batch_size, epochs, inference_steps, and parallel_sampling_number. While the model can handle any graph scale after one training, we adjust settings for different training sets, detailed in our open-source code. Notably, GDSG uses very few diffusion (e.g., 200) and inference steps (e.g., 5), unlike the thousands of steps in other works [32], [36]. This efficiency is due to the lower-dimensional scale and higher certainty of our problem compared to image generation.

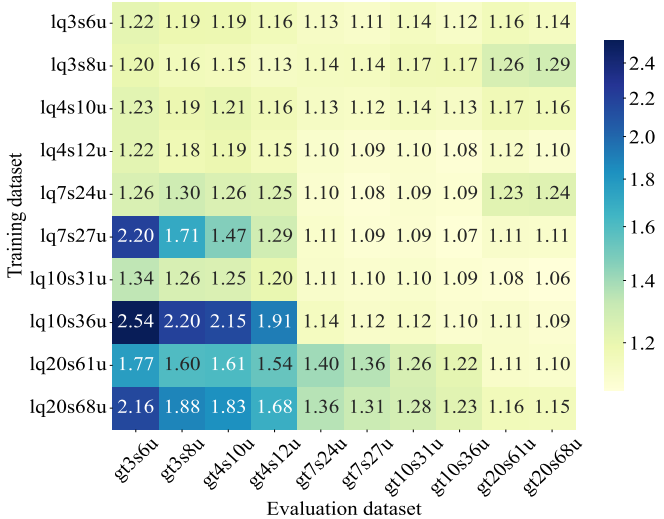


Fig. 5. The performance Exceed_ratio of GDSG (GNN padding edge not handled).

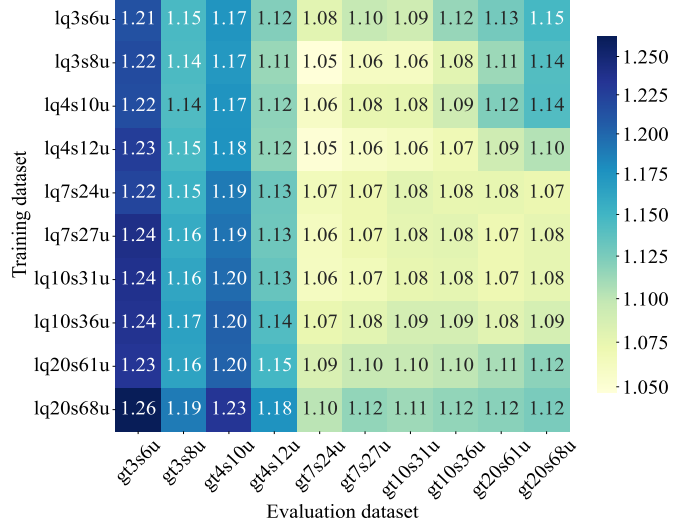


Fig. 6. The performance Exceed_ratio of GDSG (GNN padding edge handled).

3) *Metrics*: We aim to minimize the weighted cost, so we use the Exceed_ratio of output solution cost to the testing label cost as the metric. On the optimal testing set, the Exceed_ratio should be close to 1, with smaller values being better.

4) *Baselines*: We use five baseline methods: the heuristic algorithm with the MCMF algorithm, which is the tool used to generate the suboptimal datasets for GDSG and other baselines, and the corresponding code has also been open-sourced; the discriminative GNN (DiGNN) with the same neural network structure as our GDSG; and MTFNN [22], an off-the-shelf multi-task learning DNN method; DIFUSCO [36] and T2T [37] are also included as latest known methods that use diffusion generation for combinatorial optimization. For all experiments, each hyperparameter for a given model and training set is fixed by default (details are in the open source). For the following sections, the neural network settings

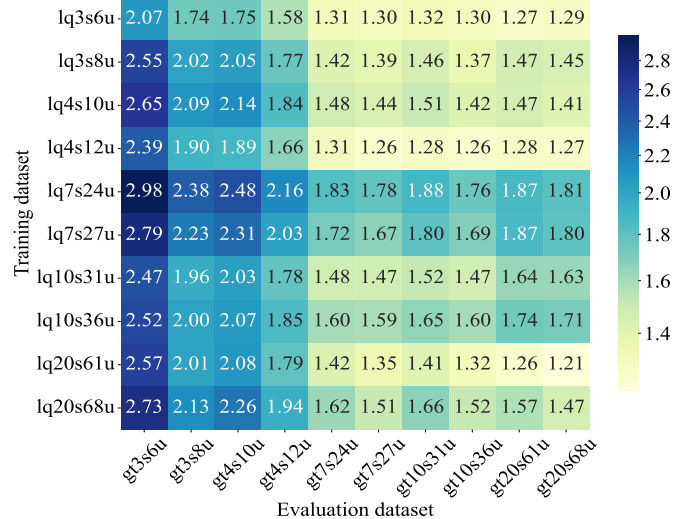


Fig. 7. The performance Exceed_ratio of DiGNN (GNN padding edge handled).

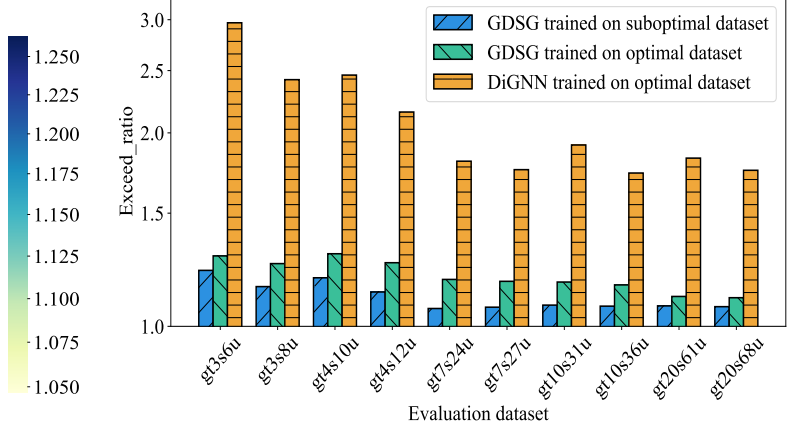


Fig. 8. Performance comparison of three trained models: GDSG trained on a suboptimal dataset (lq7s24u, 80000 samples), GDSG trained on an optimal dataset (gt3s6u, 2000 samples) and DiGNN trained on an optimal dataset (gt3s6u, 2000 samples).

for GDSG and DiGNN are identical. GDSG shares the same diffusion-related hyperparameter settings as DIFUSCO and T2T. All dataset generation is done on an Intel i7-13700F, and all model training and testing are performed on an RTX 4090.

B. Empirical Verification for Theory

Based on (Eq. (12), Eq. (13)), we demonstrate $\mathbb{E}(q(\theta^n))$ for three cases in both discrete and continuous diffusion: $N = 1, 10, 20$. We set the possible values for the unknown variables in the equation under the assumptions in Sec. III-B. For discrete solutions, we set $\epsilon = 0.1$. For continuous solutions, we uniformly set $y_i = 1$, $\epsilon = 0.1$, $\gamma_i = 0.04$, and $\delta = 0.1$. The expected value of $\mathbb{E}(q(\theta^n))$ is then computed, resulting in Fig. 3. We use dotted lines of the same color as the curves to mark the corresponding lower bound on the number of samples n in Eq. (12) and Eq. (13). Here we consider $\mathbb{E}(q(\theta^n)) > 0.95$ as $\mathbb{E}(q(\theta^n)) \approx 1$. As n increases, the expectation approaches

TABLE I
PERFORMANCE COMPARISON OF EXCEED_RATIO BETWEEN GDSG AND BASELINES.

Evaluation Dataset	MTFNN	HEU	DiGNN	DIFUSCO	T2T	GDSG (Ours)
gt3s6u	83.44	1.22	2.07	1.22	-	1.22
gt3s8u	288.93	1.17	1.74	1.18	-	1.15
gt4s10u	3493837.38	1.20	1.75	1.19	-	1.19
gt4s12u	225.07	1.17	1.58	1.15	-	1.13
gt7s24u	804.12	1.13	1.31	1.10	-	1.07
gt7s27u	407798.51	1.14	1.30	1.09	-	1.07
gt10s31u	2672.08	1.14	1.32	1.10	-	1.08
gt10s36u	230.47	1.15	1.30	1.08	-	1.08
gt20s61u	1272.67	1.15	1.27	1.12	-	1.08
gt20s68u	4517.63	1.18	1.29	1.10	-	1.07

1. Although some unknown variables are assigned assumed values, Fig. 3 visually illustrates the convergence process of sampling from the high-quality solution distribution and the associated influencing factors.

Additionally, for the unknown variables in Eq. 9, which refer to the model's generation data variance, we use empirical calculations based on the existing model outputs. The trained model is used to repeat 1000 inferences on the same input and count the variance of the output θ s, which is on the order of 10^{-4} . Therefore, $\frac{\sigma^2}{\epsilon^2}$ can be small, e.g., $\frac{\sigma^2}{\epsilon^2} = 0.01$ if $\sigma^2 = 0.0001, \epsilon = 0.1$. Although this is not a perfect theoretical conclusion, it demonstrates the small, even almost negligible, gap between the learned distribution and the optimal distribution.

C. Multi-Task Orthogonality

As we try to address discrete diffusion and continuous diffusion in a single model, we should ensure the gradient vectors of the two tasks are orthogonal so there is no negative competition between the two tasks during training [57], [58]. The non-orthogonality of the gradient vectors of two tasks often leads to inferior convergence. Considering this kind of risk, we track the gradient directions of the related parameters for both tasks throughout the training process of our model and the baseline, DiGNN, with the same neural network structure. Specifically, we perform backpropagation of the loss for each task at each training iteration across multiple epochs. Then we extract a high-dimension vector, which contains the information from the parameter updating gradient, of each parameter of representative network layers (input layer, edge feature embedding layer, node feature embedding layer, etc). Then we compute the cosine of the angle between the update vectors of the two tasks to quantify their orthogonality. The results are shown in Fig. 4.

It is observed that in GDSG, the two tasks show a high degree of orthogonality with cosine values approaching 1 and orthogonal gradient proportions approaching 100%, which is in sharp contrast to the baseline. For DiGNN, it shows poor orthogonality with cosine values far away from 1 and orthogonal gradient proportions always less than 10%. Furthermore, GDSG has a small variance (the maximum magnitude is 4

while DiGNN has a large variance (the minimum magnitude is 7), which means that the gradient angles of GDSG are more concentrated in orthogonality. This advantage is benefit from the configuration of the loss function of diffusion. Therefore, the simultaneous training of the two tasks in a single GDSG model does not impede each other, which avoids any degradation of model performance.

D. GDSG vs DiGNN on Effectiveness and Generalization

This section compares GDSG and DiGNN to illustrate the improvement brought by diffusion generation. We train 10 GDSG models and 10 DiGNN models on the 10 suboptimal training sets and evaluate them on the 10 optimal testing sets. In Fig. 6, GDSG's Exceed_ratio on most testing sets is below 1.1, with a few reaching 1.2, indicating near-optimal performance. This significantly outperforms DiGNN, which has a minimum Exceed_ratio over 1.2 (Fig. 7). Both models perform worse on scales with 3 and 4 servers due to the denser input graphs causing over-smoothing [55] in deep iterative GNNs. The slightly poorer performance at the corners and edges of the heatmaps suggests some generalization issues with GNN implementation. Overall, despite some engineering flaws, GDSG trained on suboptimal datasets not only approaches the optimal solution but also surpasses the discriminative model and shows good generalization.

We also build 4 optimal training sets of small-scale problems, each with 2000 samples, to train 4 GDSG models and 4 DiGNN models. We compare the best-performing GDSG from Fig. 6 with the best GDSG and DiGNN trained on the optimal dataset. Fig. 8 shows that GDSG outperforms DiGNN even with the same optimal dataset, and suboptimal training with sufficient samples is consistently better. For the models trained on the truth datasets, GDSG can save up to 56.63% (GDSG trained on gt3s6u vs DiGNN trained on gt3s6u evaluated on gt3s6u) of the total target cost. This demonstrates that GDSG can effectively learn from both suboptimal and optimal samples.

Comparing Fig. 5 and Fig. 6, our GNN uses the generalization improvements with the maximum improvement exceeding 86% (1.166 vs 2.195 evaluated on gt3s8u). Other generalization improvement results are available in open source. GDSG's

running time scales with problem size, taking about 0.4 seconds per inference in the gt20s68u test and 0.03 seconds in the gt3s6u test. This is comparable to other common deep learning methods, meeting the real-time requirements for network optimization. In short, the GDSG model's outstanding performance shows how effectively it combines solution space parametrization with diffusion generative learning on suboptimal training sets.

E. Comparison with Baseline Schemes

We compare the Exceed_ratio of GDSG with all baselines in Table I. MTFNN, which can only process vector data and lacks graph understanding capability, can train only one model per test scale, resulting in very poor performance. In some problems, MTFNN's Exceed_ratio reaches tens of thousands due to the large data volume and high communication costs of computationally intensive tasks. Incorrect offloading by MTFNN leads to extremely high total cost. In comparison, HEU and DiGNN can achieve relatively better results, and GDSG also outperforms HEU and DiGNN across the board. Although HEU uses the MCMF algorithm to ensure the optimal offloading decision for a given computational resource allocation, its heuristic initialization of resource allocation cannot guarantee optimality, leading to suboptimal results. Furthermore, GDSG reduces the total target cost by up to 41.07% (GDSG trained on lq7s24u vs DiGNN trained on lq3s6u evaluated on gt3s6u).

DIFUSCO performs relatively worse than GDSG, with the performance gap primarily due to the lack of consideration for padding edges in the GNN. On the other hand, T2T introduces automatic gradient computation of the target optimization function's gradient during the denoising process. While this is computable for TSP and MIS problems in the original work, our computation offloading objective function is non-differentiable, making gradients unavailable. As a result, T2T is not applicable to MEC network optimization problems like ours.

VI. CONCLUSION AND DISCUSSION

In this study, we introduce GDSG, a model for generating solutions based on graph diffusion, especially delivering optimization solution generation capabilities that are robust to training data. We focus on NP-hard optimization problems in MEC networks that lack efficient approximation algorithms, using the widely prevalent multi-server multi-user computation offloading problem as a concrete scenario. Our model converts network optimization problems into distribution learning through a defined parameterization of the solution space, which supports learning from suboptimal training sets that can be obtained efficiently. The paper provides important findings and explanations that advocate the application of generative models in solution generation. This application offers a cohesive problem formulation and model framework for network optimization. Furthermore, we construct a database for the multi-server multi-user computation offloading (MSCO) optimization problem, including suboptimal training sets, optimal training sets for a small number of small-scale problems,

and optimal test sets. Through our experiments, GDSG has shown superior performance compared to baseline methods, whether on the suboptimal training set or the optimal training set. The proposed GDSG approach disrupts the current trend in learning-based network optimization methods that rely heavily on extensive ground-truth datasets, thereby reducing the reliance on real optimal datasets.

We have considered some future directions of this work, one of which is ensuring that generated solutions satisfy the constraints of optimization problems through more explicit mechanisms. Additionally, the presence of numerous unknown variables in the theoretical framework means that comprehensive conclusions on convergence or data requirements remain room for further investigation.

REFERENCES

- [1] Y. Mao, C. You, J. Zhang, K. Huang, and K. B. Letaief, "A Survey on Mobile Edge Computing: The Communication Perspective," *IEEE Communications Surveys & Tutorials*, vol. 19, no. 4, pp. 2322–2358, 2017.
- [2] P. Mach and Z. Becvar, "Mobile Edge Computing: A Survey on Architecture and Computation Offloading," *IEEE Communications Surveys & Tutorials*, vol. 19, no. 3, pp. 1628–1656, 2017.
- [3] A. Coletta, F. Giorgi, G. Maselli, M. Prata, D. Silvestri, J. Ashdown, and F. Restuccia, "A2-UAV: Application-Aware Content and Network Optimization of Edge-Assisted UAV Systems," in *Proc. of IEEE INFOCOM*, 2023, pp. 1–10.
- [4] C. Zhan, H. Hu, S. Mao, and J. Wang, "Energy-Efficient Trajectory Optimization for Aerial Video Surveillance under QoS Constraints," in *Proc. of IEEE INFOCOM*, 2022, pp. 1559–1568.
- [5] S. Chai and V. K. N. Lau, "Multi-UAV Trajectory and Power Optimization for Cached UAV Wireless Networks With Energy and Content Recharging-Demand Driven Deep Learning Approach," *IEEE JSAC*, vol. 39, no. 10, pp. 3208–3224, 2021.
- [6] C. Zhao, J. Liu, M. Sheng, W. Teng, Y. Zheng, and J. Li, "Multi-UAV Trajectory Planning for Energy-Efficient Content Coverage: A Decentralized Learning-Based Approach," *IEEE JSAC*, vol. 39, no. 10, pp. 3193–3207, 2021.
- [7] D. C. Nguyen, S. Hosseinalipour, D. J. Love, P. N. Pathirana, and C. G. Brinton, "Latency Optimization for Blockchain-Empowered Federated Learning in Multi-Server Edge Computing," *IEEE JSAC*, vol. 40, no. 12, pp. 3373–3390, 2022.
- [8] N. Karakoç, A. Scaglione, M. Reisslein, and R. Wu, "Federated Edge Network Utility Maximization for a Multi-Server System: Algorithm and Convergence," *IEEE/ACM TON*, vol. 30, no. 5, pp. 2002–2017, 2022.
- [9] X. Cao, B. Yang, C. Huang, C. Yuen, M. D. Renzo, D. Niyato, and Z. Han, "Reconfigurable Intelligent Surface-Assisted Aerial-Terrestrial Communications via Multi-Task Learning," *IEEE JSAC*, vol. 39, no. 10, pp. 3035–3050, 2021.
- [10] B. Di, H. Zhang, L. Song, Y. Li, Z. Han, and H. V. Poor, "Hybrid Beamforming for Reconfigurable Intelligent Surface based Multi-User Communications: Achievable Rates With Limited Discrete Phase Shifts," *IEEE JSAC*, vol. 38, no. 8, pp. 1809–1822, 2020.
- [11] W. Feng, J. Tang, Q. Wu, Y. Fu, X. Zhang, D. K. C. So, and K.-K. Wong, "Resource Allocation for Power Minimization in RIS-Assisted Multi-UAV Networks With NOMA," *IEEE TCOM*, vol. 71, no. 11, pp. 6662–6676, 2023.
- [12] W. Mei and R. Zhang, "Joint Base Station and IRS Deployment for Enhancing Network Coverage: A Graph-Based Modeling and Optimization Approach," *IEEE TWC*, vol. 22, no. 11, pp. 8200–8213, 2023.
- [13] X. Zhang, B. Yang, Z. Yu, X. Cao, G. C. Alexandropoulos, Y. Zhang, M. Debbah, and C. Yuen, "Reconfigurable Intelligent Computational Surfaces for MEC-Assisted Autonomous Driving Networks: Design Optimization and Analysis," *IEEE TITS*, pp. 1–18, 2024.
- [14] Z. Lv, D. Chen, and Q. Wang, "Diversified Technologies in Internet of Vehicles Under Intelligent Edge Computing," *IEEE TITS*, vol. 22, no. 4, pp. 2048–2059, 2021.
- [15] T. Z. H. Ernest and A. S. Madhukumar, "Computation Offloading in MEC-Enabled IoT Networks: Average Energy Efficiency Analysis and Learning-Based Maximization," *IEEE TMC*, vol. 23, no. 5, pp. 6074–6087, 2024.

[16] G. Sun, Z. Wang, H. Su, H. Yu, B. Lei, and M. Guizani, "Profit Maximization of Independent Task Offloading in MEC-Enabled 5G Internet of Vehicles," *IEEE TITS*, vol. 25, no. 11, pp. 16 449–16 461, 2024.

[17] P. Dai, K. Hu, X. Wu, H. Xing, and Z. Yu, "Asynchronous Deep Reinforcement Learning for Data-Driven Task Offloading in MEC-Empowered Vehicular Networks," in *Proc. of IEEE INFOCOM*, 2021, pp. 1–10.

[18] X. He, X. Zhuge, F. Dang, W. Xu, and Z. Yang, "DeepScheduler: Enabling Flow-Aware Scheduling in Time-Sensitive Networking," in *Proc. of IEEE INFOCOM*, 2023, pp. 1–10.

[19] K. Rusek, J. Suárez-Varela, P. Almasan, P. Barlet-Ros, and A. Cabellos-Aparicio, "RouteNet: Leveraging graph neural networks for network modeling and optimization in SDN," *IEEE JSAC*, vol. 38, no. 10, pp. 2260–2270, 2020.

[20] T. Chen, X. Zhang, M. You, G. Zheng, and S. Lambotharan, "A GNN-based supervised learning framework for resource allocation in wireless IoT networks," *IEEE IOT*, vol. 9, no. 3, pp. 1712–1724, 2021.

[21] F. Jiang, K. Wang, L. Dong, C. Pan, W. Xu, and K. Yang, "Deep-learning-based joint resource scheduling algorithms for hybrid MEC networks," *IEEE IOT*, vol. 7, no. 7, pp. 6252–6265, 2019.

[22] B. Yang, X. Cao, J. Bassey, X. Li, and L. Qian, "Computation offloading in multi-access edge computing: A multi-task learning approach," *IEEE TMC*, vol. 20, no. 9, pp. 2745–2762, 2020.

[23] Liang, Ruihuai and Yang, Bo and Yu, Zhiwen and Cao, Xuelin and Ng, Derrick Wing Kwan and Yuen, Chau, "A multi-head ensemble multi-task learning approach for dynamical computation offloading," in *Proc. of IEEE GLOBECOM*, 2023, pp. 6079–6084.

[24] K. Li, M. Tao, and Z. Chen, "Exploiting Computation Replication in Multi-User Multi-Server Mobile Edge Computing Networks," in *Proc. of IEEE GLOBECOM*, 2018, pp. 1–7.

[25] H. Zhang, X. Ma, X. Liu, L. Li, and K. Sun, "GNN-Based Power Allocation and User Association in Digital Twin Network for the Terahertz Band," *IEEE JSAC*, 2023.

[26] E. Zelikman, Y. Wu, J. Mu, and N. D. Goodman, "STaR: self-taught reasoner bootstrapping reasoning with reasoning," in *Proc. of NeurIPS*, 2024.

[27] P. Ma, T.-H. Wang, M. Guo, Z. Sun, J. B. Tenenbaum, D. Rus, C. Gan, and W. Matusik, "LLM and Simulation as Bilevel Optimizers: A New Paradigm to Advance Physical Scientific Discovery," in *Proc. of ICML*, vol. 235, 21–27 Jul 2024, pp. 33 940–33 962. [Online]. Available: <https://proceedings.mlr.press/v235/ma24m.html>

[28] X. Du, Y. Sun, X. Zhu, and Y. Li, "Dream the impossible: outlier imagination with diffusion models," in *Proc. of NeurIPS*, 2024.

[29] L. Zhang, A. Rao, and M. Agrawala, "Adding Conditional Control to Text-to-Image Diffusion Models," in *Proc. of ICCV*, 2023, pp. 3813–3824.

[30] R. Qiu, Z. Sun, and Y. Yang, "DIMES: A Differentiable Meta Solver for Combinatorial Optimization Problems," in *Proc. of NeurIPS*, vol. 35, 2022, pp. 25 531–25 546.

[31] H. Cao, C. Tan, Z. Gao, Y. Xu, G. Chen, P.-A. Heng, and S. Z. Li, "A Survey on Generative Diffusion Models," *IEEE TKDE*, vol. 36, no. 7, pp. 2814–2830, 2024.

[32] J. Ho, A. Jain, and P. Abbeel, "Denoising Diffusion Probabilistic Models," in *Proc. of NeurIPS*, vol. 33, 2020, pp. 6840–6851.

[33] J. Ho and T. Salimans, "Classifier-free diffusion guidance," *arXiv preprint arXiv:2207.12598*, 2022.

[34] P. Dhariwal and A. Nichol, "Diffusion Models Beat GANs on Image Synthesis," in *Proc. of NeurIPS*, vol. 34, 2021, pp. 8780–8794.

[35] J. Austin, D. D. Johnson, J. Ho, D. Tarlow, and R. van den Berg, "Structured Denoising Diffusion Models in Discrete State-Spaces," in *Proc. of NeurIPS*, vol. 34, 2021, pp. 17 981–17 993.

[36] Z. Sun and Y. Yang, "DIFUSCO: Graph-based Diffusion Solvers for Combinatorial Optimization," in *Proc. of NeurIPS*, vol. 36, 2023, pp. 3706–3731.

[37] Y. Li, J. Guo, R. Wang, and J. Yan, "T2T: From Distribution Learning in Training to Gradient Search in Testing for Combinatorial Optimization," in *Proc. of NeurIPS*, vol. 36, 2023, pp. 50 020–50 040.

[38] H. Du, R. Zhang, Y. Liu, J. Wang, Y. Lin, Z. Li, D. Niyato, J. Kang, Z. Xiong, S. Cui, B. Ai, H. Zhou, and D. I. Kim, "Enhancing Deep Reinforcement Learning: A Tutorial on Generative Diffusion Models in Network Optimization," *IEEE Communications Surveys & Tutorials*, pp. 1–1, 2024.

[39] R. Liang, B. Yang, Z. Yu, B. Guo, X. Cao, M. Debbah, H. V. Poor, and C. Yuen, "DiffSG: A Generative Solver for Network Optimization with Diffusion Model," 2024. [Online]. Available: <https://arxiv.org/abs/2408.06701>

[40] J. Wang, H. Du, Y. Liu, G. Sun, D. Niyato, S. Mao, D. I. Kim, and X. Shen, "Generative AI based Secure Wireless Sensing for ISAC Networks," 2024. [Online]. Available: <https://arxiv.org/abs/2408.11398>

[41] G. Sun, W. Xie, D. Niyato, F. Mei, J. Kang, H. Du, and S. Mao, "Generative AI for Deep Reinforcement Learning: Framework, Analysis, and Use Cases," 2024. [Online]. Available: <https://arxiv.org/abs/2405.20568>

[42] H. Du, Z. Li, D. Niyato, J. Kang, Z. Xiong, H. Huang, and S. Mao, "Diffusion-Based Reinforcement Learning for Edge-Enabled AI-Generated Content Services," *IEEE TMC*, vol. 23, no. 9, pp. 8902–8918, 2024.

[43] Y. Liu, H. Du, D. Niyato, J. Kang, Z. Xiong, D. I. Kim, and A. Jamaliour, "Deep Generative Model and Its Applications in Efficient Wireless Network Management: A Tutorial and Case Study," *IEEE Wireless Communications*, vol. 31, no. 4, pp. 199–207, 2024.

[44] E. Yaacoub and Z. Dawy, "A survey on uplink resource allocation in OFDMA wireless networks," *IEEE Communications Surveys & Tutorials*, vol. 14, no. 2, pp. 322–337, 2011.

[45] M. Salem, A. Adinoyi, M. Rahman, H. Yanikomeroglu, D. Falconer, Y.-D. Kim, E. Kim, and Y.-C. Cheong, "An overview of radio resource management in relay-enhanced OFDMA-based networks," *IEEE Communications Surveys & Tutorials*, vol. 12, no. 3, pp. 422–438, 2010.

[46] X. Chen, "Decentralized computation offloading game for mobile cloud computing," *IEEE TPDS*, vol. 26, no. 4, pp. 974–983, 2014.

[47] T. D. Burd and R. W. Brodersen, "Processor design for portable systems," *Journal of VLSI signal processing systems for signal, image and video technology*, vol. 13, no. 2, pp. 203–221, 1996.

[48] L. Beal, D. Hill, R. Martin, and J. Hedengren, "GEKKO Optimization Suite," *Processes*, vol. 6, no. 8, p. 106, 2018.

[49] J. G. Saw, M. C. Yang, and T. C. Mo, "Chebyshev inequality with estimated mean and variance," *The American Statistician*, vol. 38, no. 2, pp. 130–132, 1984.

[50] D. Kingma and R. Gao, "Understanding Diffusion Objectives as the ELBO with Simple Data Augmentation," in *Proc. of NeurIPS*, vol. 36, 2023, pp. 65 484–65 516.

[51] D. Kingma, T. Salimans, B. Poole, and J. Ho, "Variational Diffusion Models," in *Proc. of NeurIPS*, vol. 34, 2021, pp. 21 696–21 707.

[52] E. Hoogeboom, D. Nielsen, P. Jaini, P. Forré, and M. Welling, "Argmax Flows and Multinomial Diffusion: Learning Categorical Distributions," in *Proc. of NeurIPS*, vol. 34, 2021, pp. 12 454–12 465.

[53] T. Chen, R. Zhang, and G. Hinton, "Analog bits: Generating discrete data using diffusion models with self-conditioning," *arXiv preprint arXiv:2208.04202*, 2022.

[54] C. K. Joshi, Q. Cappart, L.-M. Rousseau, and T. Laurent, "Learning the travelling salesperson problem requires rethinking generalization," *Constraints*, vol. 27, no. 1, pp. 70–98, 2022.

[55] V. P. Dwivedi, C. K. Joshi, A. T. Luu, T. Laurent, Y. Bengio, and X. Bresson, "Benchmarking graph neural networks," *MIT Press JMLR*, vol. 24, no. 43, pp. 1–48, 2023.

[56] X. Guo and L. Zhao, "A systematic survey on deep generative models for graph generation," *IEEE TPAMI*, vol. 45, no. 5, pp. 5370–5390, 2022.

[57] L. Liu, Y. Li, Z. Kuang, J.-H. Xue, Y. Chen, W. Yang, Q. Liao, and W. Zhang, "Towards Impartial Multi-task Learning," in *Proc. of ICLR*, 2021.

[58] T. Yu, S. Kumar, A. Gupta, S. Levine, K. Hausman, and C. Finn, "Gradient Surgery for Multi-Task Learning," in *Proc. of NeurIPS*, vol. 33, 2020, pp. 5824–5836.

[59] Z. Chen, J. Ngiam, Y. Huang, T. Luong, H. Kretzschmar, Y. Chai, and D. Anguelov, "Just Pick a Sign: Optimizing Deep Multitask Models with Gradient Sign Dropout," in *Proc. of NeurIPS*, vol. 33. Curran Associates, Inc., 2020, pp. 2039–2050.

[60] H. Go, Y. Lee, S. Lee, S. Oh, H. Moon, and S. Choi, "Addressing Negative Transfer in Diffusion Models," in *Proc. of NeurIPS*, vol. 36, 2023, pp. 27 199–27 222.

[61] H. Ye and D. Xu, "DiffusionMTL: Learning Multi-Task Denoising Diffusion Model from Partially Annotated Data," in *Proc. of CVPR*, 2024, pp. 27 960–27 969.

[62] H. He, C. Bai, K. Xu, Z. Yang, W. Zhang, D. Wang, B. Zhao, and X. Li, "Diffusion Model is an Effective Planner and Data Synthesizer for Multi-Task Reinforcement Learning," in *Proc. of NeurIPS*, vol. 36, 2023, pp. 64 896–64 917.

[63] J. Song, C. Meng, and S. Ermon, "Denoising Diffusion Implicit Models," in *Proc. of ICLR*, 2021.